

A multi-object, multi-field spectrometer and imager for a European ELT

Chris Evans^a, Colin Cunningham^a, Eli Atad-Etchedgui^a, Jeremy Allington-Smith^b, Francois Assémat^b, Gavin Dalton^{c,d}, Peter Hastings^a, Timothy Hawarden^a, Isobel Hook^c, Rob Ivison^a, Simon Morris^b, Suzanne Ramsay Howat^a, Mel Strachan^a and Stephen Todd^a

^aUK Astronomy Technology Centre, Royal Observatory, Blackford Hill, Edinburgh, EH9 3HJ, UK;

^bDept. of Physics, University of Durham, South Road, DH1 3LE, UK;

^cDept. of Astrophysics, Denys Wilkinson Building, Keble Road, Oxford, OX1 3RH, UK;

^dSpace Science & Technology Dept., CCLRC Rutherford Appleton Lab., Chilton, OX11 0QX, UK

ABSTRACT

One of the highlights of the European ELT Science Case book is the study of resolved stellar populations, potentially out to the Virgo Cluster of galaxies. A European ELT would enable such studies in a wide range of unexplored distant environments, in terms of both galaxy morphology and metallicity. As part of a small study, a revised science case has been used to shape the conceptual design of a multi-object, multi-field spectrometer and imager (MOMSI). Here we present an overview of some key science drivers, and how to achieve these with elements such as multiplex, AO-correction, pick-off technology and spectral resolution.

1. INTRODUCTION

The possibility of studying resolved stellar populations in the Virgo cluster of galaxies (at ~ 16 Mpc) was one of the foremost sections of the OPTICON Science Case for a European Extremely Large Telescope¹ (E-ELT). A very large primary aperture combined with improved spatial resolution over that from 10-m class facilities offers immense potential for studies of stellar populations in galaxies, from the edge of the Local Group right out to Virgo.

As part of the FP6 Instrument Small Studies for an E-ELT we have revisited the science case and developed an initial design concept for a multi-object, multi-field spectrometer and imager (MOMSI). As the plans for an E-ELT have evolved, the relative strengths of different science cases have also evolved. Here we present potential studies of resolved stellar populations that would benefit from an E-ELT, especially when combined with significant wavefront correction from an adaptive optics (AO) system. Due to the technical drive toward the near-IR (in which the AO correction is more effective) a MOMSI-type instrument would obviously also benefit studies of galaxy evolution and other programmes at high redshift; for completeness we highlight a couple of areas to which MOMSI could contribute. Although less demanding in terms of the required AO-correction, we note that one of the most compelling science cases for a multi-object near-IR spectrograph on an ELT will most likely concern the follow-up of faint galaxies discovered by the *James Webb Space Telescope* (JWST).

2. SCIENCE CASE

Before discussing specific cases it is worth identifying a more general requirement from the desire to study resolved stellar populations with an E-ELT. The correction from adaptive optics (AO) becomes more effective at longer wavelengths; the reality of significant AO-correction in the optical domain may yet be some time ahead. Many conceivable projects to study resolved stellar populations are still dependent on optical diagnostics at some level – some of this is perhaps historical, but it is also true that there are generally fewer diagnostics in the near-IR, both photometrically and spectroscopically. In this context, access to the *I* and *Z* passbands would be of significant benefit. Photometry in these bands adds significant leverage on age and metallicity determinations of e.g. the main-sequence turn-off in old populations. Moreover, spectroscopy in the *I*-band region gives access to the Calcium II triplet (CaT), with rest wavelengths of 850, 854, and 866 nm. In contemporary studies of stellar kinematics the CaT is the fundamental diagnostic feature, and is not covered by the other E-ELT Small Studies in progress. Other spectral lines of interest also lie in this region e.g. the Paschen series of hydrogen.

In Sections 2.1 to 2.5 we discuss five specific areas of research that require an instrument such as MOMSI to satisfy the scientific aims. Here we have focussed on applications requiring spectroscopy. The science case for imaging² would make somewhat different demands on the AO system – this will be more fully explored in future point-design studies.

2.1. Stellar kinematics and galactic archaeology

Over the past decade new multi-object instrumentation has enabled the study of so-called ‘galaxy archaeology’. This involves mapping the kinematics of the stellar content of the Milky Way and nearby galaxies to determine the sub-components of their structure, then combining the velocity information with abundance analyses of selected stars. This fossil record of a galaxy can then be used to investigate the star-formation history, chemical evolution, evidence for past merger activity, and the formation of components such as bulges etc. In essence, *exploring mass assembly at low-redshift*. A number of projects are currently exploring the outer components of the Milky Way (e.g. the RAVE consortium³, the proposed AAOmega ARGUS programme, the proposed Gemini-WFMOS instrument), with others focussing their efforts on M31 and its satellites⁴.

One of the principal limiting factors in ongoing studies remains the lack of accessible systems – how typical are the processes that we see in the Milky Way and the Andromeda group? With deployable integral field units (IFUs), MOMSI will be able to examine the kinematic structure of stellar populations in a wide range of galaxies. In particular, probing the less-crowded, outer-regions of a galaxy can provide some of the most revealing discoveries, as illustrated by the discovery of relatively faint structures around M31⁵. MOMSI will be able to study the kinematics of the most luminous stars in the outer regions of galaxies in the Virgo Cluster, as well as obtaining first-order estimates of their chemical compositions. With the benefit of a large primary aperture, studies of the halo populations in dark-matter dominated galaxies at the edge of the Local Group such as NGC 3109⁶ will also become feasible.

2.2. Clusters and starbursts

M82 is the nearest starburst galaxy, with considerable ongoing star formation. Much of this is seen to be occurring in young, very compact star clusters, usually referred to as super star clusters (SSCs). With the aim of understanding significant star-formation in the early Universe, spectral synthesis techniques have been applied to SSCs in M82 to understand their mass functions, and the feedback of ionizing photons into the local intercluster medium.

A ‘top-heavy’ mass function was found for an SSC in M82⁷, leading to suggestions of an abnormal initial mass function (IMF) therein. Such conclusions are still widely debated. For instance, no evidence for similar behaviour at low-masses is seen in an SSC in NGC 1705 at 5 Mpc⁸. Resolved (or near-resolved) observations with MOMSI of such clusters would enable the true stellar population to be determined, allowing studies of the IMF in each cluster, and the overall cluster mass function that modulates the IMF. Given the large quantity of dust and gas present in these compact regions, observations in the *K* band will be crucial.

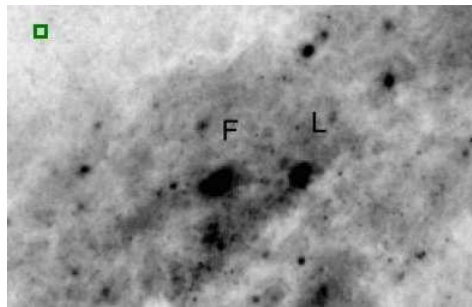


Figure 1. Super star clusters in M82 from F814W observations with WFPC2 on the *HST* (from Smith & Gallagher, 2001). The on-sky footprint of the MOMSI IFUs ($\sim 0.4 \times 0.4''$) is marked with the solid-lined box at the top left of the image. Multi-IFU observations in a galaxy such as M82 are perfect targets for an ELT.

2.3. Stellar astrophysics in new environments

One of the main drivers in stellar astrophysics over the past decade has been to understand the role of metallicity (i.e. abundance of metallic species) and environment on stellar evolution. Much of this has been motivated by a desire to better understand the evolution and formation of stars in the early Universe. New large-scale, high-resolution stellar surveys in the Galaxy and Magellanic Clouds⁹ have statistically meaningful samples to rigorously examine the dependence of physical

parameters, abundance enhancements and rotation rates on environment. Meanwhile, intermediate-resolution observations of the most visually luminous stars (which are A-type supergiants) have pushed further out to the edge of the Local Group, finding galaxies with lower metal abundances, e.g. Sextans A¹⁰.

The high-resolution mode of MOMSI would provide observations of large samples of the most massive stars in systems such as Sextans A, and beyond. This would test theoretical model atmospheres and stellar feedback in an unexplored metallicity regime – of interest in the context of the first stars in the Universe (so-called Population III stars). Similar surveys of red giants and stars on the asymptotic giant branch (AGBs) would also be of considerable interest to the community. Theoretical modeling of lines in the near-IR has advanced in recent years¹¹ and lack of access to optical diagnostics would not hamper such efforts.

The direct descendents of massive O-type stars are Wolf-Rayet (WR) stars. New studies have discussed the metallicity dependence of their outflows^{12,13}, and they have attracted interest as the likely precursors of some long gamma-ray bursts in low metallicity systems¹⁴. The discovery that I Zw 18 is a very metal-poor, young galaxy¹⁵ provides an exciting prospect in the era of ELTs. Spectroscopic observations of WR stars in systems such as I Zw 18 would enable quantitative studies of metal-poor WR stars in genuinely young, star-forming galaxies. This would improve our understanding of these young and violently-evolving stars, and enhance empirical libraries used to interpret integrated spectra of distant WR galaxies.

2.4. Mass assembly at high redshift

The majority of stellar mass is believed to build-up in galaxies between $z \sim 1-3$. Significantly massive components are seen within some galaxies¹⁶, and the optical morphology of sub-mm galaxies is found to be wide-ranging¹⁷. VLT-KMOS will measure spatially-averaged rotation curves for some of these galaxies but will be limited by spatial resolution, leading to uncertainties in the inferred properties. The long-standing debate regarding secular (i.e. external events) versus passive evolution of such galaxies will likely be better understood by the time an E-ELT is built. Nevertheless, high spatial resolution observations of these systems with MOMSI would probe unprecedented scales of distant galaxies – investigating both their dynamical structure and chemical compositions.

2.5. Super-massive blackholes and their hosts

Massive black holes are ubiquitous components of galaxies, with their mass (M_{BH}) related to the stellar mass of the surrounding bulge/spheroid^{18,19} (the Magorrian relation). M_{BH} and the luminosity-weighted line-of-sight velocity dispersion (σ) are also found to be correlated²⁰. Both the Magorrian and $M_{\text{BH}} - \sigma$ correlations represent a fossil record of past activity and imply that central black hole mass is determined by, and closely related to, the bulge properties of the host galaxy. Both relations are well constrained, with uncertainties of only 0.3 dex, largely attributable to measurement errors. Many plausible models have been put forward to explain the relations, but it is clear that a physical understanding of the interaction between a black hole, its accretion disk and the inner bulge of its host galaxy is required. With high spatial-resolution MOMSI will be able to study the dynamics of the inner regions of targeted host galaxies, at wavelengths relatively impervious to foreground obscuration.

For a sub-sample of relatively local galaxies¹⁹, this is a very compelling, mono-IFU science case – especially for disentangling the stellar population around the central black hole in M31²¹. Studying the cores of multiple galaxies in more distant galaxy clusters is also a possibility, e.g. in Abell 2443 at $z \sim 0.1$ ²².

3. BASELINE REQUIREMENTS

Following the assumed baseline of the current European working groups, we adopt a 42-m primary aperture. In Table 1 we summarize the specifications of MOMSI. Each of these is now discussed in turn:

- **Patrol field:** The patrol field for MOMSI is 2×2 arcmin. This choice is primarily driven by the spatial extent of galaxies in the Virgo Cluster, with the proposed field encompassing roughly a quadrant of a major spiral such as M100 (see Figure 2). For smaller galaxies in Virgo it would be possible to simply pick-off sample regions around the outer parts of the whole galaxy in one exposure.

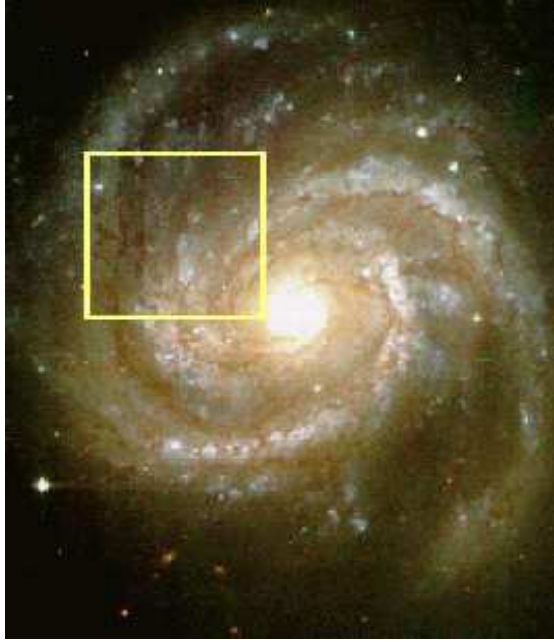


Figure 2. M100 in the Virgo Cluster. This is a combined *BVI* image from the Isaac Newton Telescope (INT) in La Palma, with north-east at the top left. The solid-lined box indicates the MOMSI patrol field of 2×2 arcmin.

- **Spectroscopic pick-off FOV:** The SSCs in M82 (Figure 1) are well-matched by a spectroscopic pick-off of ~ 0.4 - $0.5''$ squared. Such scales are also comparable to the typical half-light radii of $z \sim 3$ galaxies (of order 0.2 - $0.3''$ ²³). Allowing for a conservative inter-slice gap, a 2k array detector can accommodate 40 slices in each IFU, which at 10 mas sampling gives a FOV of $0.4'' \times 0.4''$. Slightly larger fields could be useful but, if working at the highest spatial-resolution, would require larger (or additional) detectors, image slicers etc.
- **Imaging pick-off FOV:** At 5mas sampling, $10'' \times 10''$ corresponds to a 2k array in each pick-off. To put this in context, at a distance of 16 Mpc (i.e. the Virgo Cluster) this is roughly equivalent to imaging the stellar content within a 1-degree field in the Large Magellanic Cloud, which more than adequately samples a wide range of structures.
- **Multiplex:** The stellar populations part of the science case would benefit from as large a multiplex as possible, although studies of high- z galaxies may not have sufficient source densities in a $2'$ field to complement this. Considering such arguments, in conjunction with physical space and design constraints (especially those arising from the AO-system) we adopt an approach with 20 IFU, spectroscopic pick-offs and 10 imaging pick-offs.
- **Spatial resolution:** In principle we want to fully exploit the spatial information from an E-ELT. This leads to a goal of 50% ensquared energy in 10 mas (in the *H*-band), with critical 2-pixel sampling for imaging, though this is less pressing in the spectroscopic mode.
- **Spectral resolution:** The science case requires two spectroscopic modes – ‘low-resolution’ with $R \sim 4,000$ (to resolve the sky emission lines in the near-IR) and ‘high-resolution’ with $R \sim 20,000$. The requirement for the high-resolution mode comes from the desire to determine accurate chemical abundances, using metallic lines that are often relatively weak and blended. Past experience with near-IR instruments (e.g. NIRSPEC on Keck II) has demonstrated the suitability of this resolution for accurate abundances²⁴; similarly in the optical with VLT-FLAMES²⁵.
- **Wavelength range:** *JHK* required, with *I* and *Z* bands as a goal. At $R \sim 4,000$, full coverage of a passband is required in one exposure (i.e. *J*, *H*, *K*, or *I* + *Z*). In the high-resolution mode, a 2k array detector will give coverage of ~ 0.05 to $0.2 \mu\text{m}$ in one exposure, depending on the central wavelength. This is adequate to, for example, determine abundances in cool, red giant stars which have a large number of metallic lines in the *H* band²⁴.

Table 1. Summary of baseline requirements for MOMSI.

Requirement	Imaging	Spectroscopy
Patrol field	$2' \times 2'$	
Pick-off FOV	10×10 arcsec	0.4×0.4 arcsec
Multiplex	10	20
Spatial resolution	50% of energy within 10 mas	
Spatial sampling	5 mas	
Spectral resolution	—	4,000 & 20,000
Wavelength range	(0.8) 1.0–2.5 μm	

4. MULTI-OBJECT ADAPTIVE OPTICS

The conceptual design for MOMSI relies on AO-correction from a multi-object adaptive optics (MOAO) system. Instead of correcting the whole focal plane, MOAO corrects the wavefront locally for each target. This was the adopted AO system for the proposed VLT-FALCON concept²⁶. FALCON uses several off-axis natural guide stars (NGS) to perform wavefront sensing around each scientific target. Using atmospheric tomography techniques it is possible to then compute the best commands to apply to the deformable mirror (DM) in each IFU. Scaling the concept to an E-ELT requires several laser guide stars (LGS) in order to solve for the cone effect, as well as NGS to correct for tip-tilt (and for possibly for windshake effects depending on the telescope design).

The demands of imaging and spectroscopy on the AO-correction are somewhat different. For high-quality imaging, particularly to disentangle crowded fields, parameters such as Strehl ratio and FWHM of the AO-corrected core are useful parameters. For spectroscopy, one is more concerned with achieving the maximum ensquared energy per element, rather than paying attention to the actual profile of the PSF. One method to improve the ensquared energy (thence the final signal-to-noise) is to relax the critical spatial sampling requirement such that the useful aperture (spatial pixel) on the sky is at least 10 mas (\sim the diffraction limit in the H band).

The coupling factor is defined as the fraction of the energy ensquared within the useful aperture, of a PSF centered on that aperture²⁷. Seeing limited couplings of $\sim 15\%$ are not sufficient, and ensquared energies are required of at least 30%, and preferably in the range of 40-50%. MOAO remains an unproven technique, but appears promising for an E-ELT. One of the potential problems remains how well the correction of the wavefront can be interpolated using one set of LGS (say 8-10) across the whole field, i.e. definitely outside of the isoplanatic patch on the sky. Depending on the performance of such methods, a possible scenario could be to have a constellation of lasers within the isoplanatic patch for one central pick-off, giving a significant coupling factor at the finest spatial resolution. An example (mono-IFU) science case for this could be to study the stellar population around the central black hole in M31²¹. The other pick-offs could then rely on LGS across the whole field, effectively working at coarser spatial resolution (perhaps employing multi-conjugate adaptive optics (MCAO) to correct across the whole patrol field, rather than MOAO).

5. OPTO-MECHANICAL OVERVIEW

With a complex AO system and a high-resolution spectroscopic mode, a gravity-stable instrument platform is required. In what follows we presuppose that the MOMSI instrument is located on a vertical Nasmyth platform.

5.1. Separating laser guide stars, natural guide stars, and science targets

Two approaches are possible:

- A large dichroic is placed at some distance from the Nasmyth focal plane, reflecting the science and NGS beams (0.8-2.5 μm) and transmitting the LGS that are distributed across the 2×2 arcmin field-of-view. The number of LGS and NGS is still to be fixed as it will depend on complex modelling of the AO-concept (Section 4). Shack-Hartman wave-front sensors then measure the atmospheric wavefront errors and these are fed to the DMs in each arm. This solution is attractive since it defines the interfaces precisely, but works in open loop.

- Relatively small dichroics are used in parallel beams, placed after the DMs. In this case they could be used in closed loop. However, this significantly complicates the focal plane, and likely requires dedicated LGS/NGS per pick-off. We do not consider this option further for now.

5.2. Field derotation

At Nasmyth focus, both the field and pupil rotate when the telescope tracks science targets. There are two possibilities to solve the field rotation problem. By a mechanical derotator incorporated to the interface between the telescope and the MOMSI instrument, or by an optical derotator covering the whole field-of-view. We have selected the first option since the necessary optical derotator would be enormous (2-3m). For the pupil rotation the DM could rotate, or it could be included as a software calibration when measuring the wavefront errors.

5.3. Atmospheric dispersion corrector

Although challenging, correction for atmospheric dispersion on an E-ELT is not insurmountable²⁸. A large ADC covering the whole 2×2 arcmin field-of-view is included, based on two rotating wedged prisms made of optical materials (e.g. ZnS/ZnSe) to compensate for the atmospheric chromatic aberration. If the ADC performance is not satisfactory to obtain near-diffraction limited images, small ADCs could be incorporated in the collimated beams of each pick-off arm.

5.4. Foreoptics

The focal plane adopts a similar philosophy to that used in VLT-KMOS²⁹, i.e. 20 pick-off arms will be used to select targeted sub-fields and direct the beams to 20 spectrometers. The 10 imaging pick-off arms will be longer, leading to 10 imagers beyond the spectrometers. The foreoptics are shown in Figure 3 and include two DMs to facilitate the wavefront correction from the AO system.

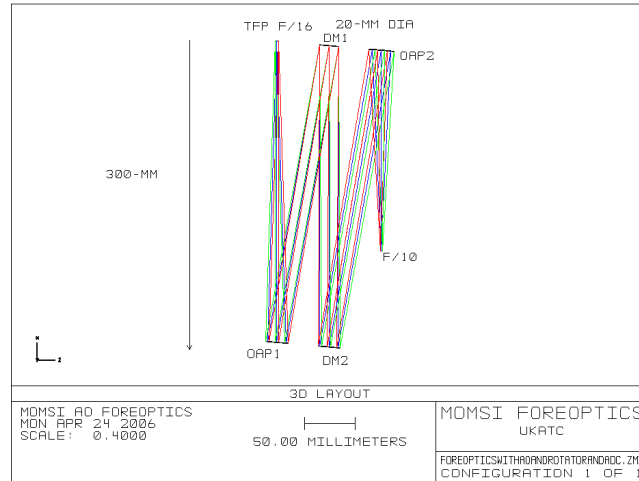


Figure 3. Foreoptics in a MOMSI pick-off arm.

5.5. IFU image slicers

The IFU is designed to slice a 0.4×0.4 arcsec image into 40 slices and reformat them to form a single slit-image at the input to the spectrograph. We propose to use a design based on those in the UKIRT 1-5 micron Imager Spectrometer (UIST)³⁰ and the Mid-infrared Instrument (MIRI)³¹ for the *JWST*.

The IFU foreoptics magnify the input image onto a slicing mirror, consisting of 40 slices. Each slice is a spherical surface, sharing a common radius of curvature. The slicing mirror forms a set of 40 pupil images that each contain the light from a single slice. A set of 40 reimaging mirrors are then used to form an image of the slices at the input focal-plane of the spectrograph, simultaneously reimaging each of the 40 separate pupils onto a single output pupil at infinity, forming a telecentric output.

The slicing mirror will consist of 40×20 mm long slices. Each slice will be reimaged to form a slit image 40 pixels long on the detector. To ensure that the spectrum is adequately (i.e. Nyquist) sampled, each slice image must be a minimum of 2 pixels wide. The physical width of the slices also determines the spatial sampling of the image on the sky. If the spatial sampling is to be equal in both dimensions then anamorphic foreoptics must be used to magnify the image by different factors in the two dimensions. The f/10 input beam will be converted to f/245 along the slices, giving a plate scale of $10\text{mas} = 0.5\text{mm} = 1\text{ pixel}$ at detector, and to f/490 across the slices, giving a plate scale of $10\text{mas} = 1\text{mm} = 1\text{ slice width}$. The reimaging optics after the slices form demagnified images of the slices, forming a telecentric output beam which is f/10 along the slices and f/20 across the slices.

Alternatively, simpler foreoptics can be used that magnify both dimensions equally, giving different spatial sampling along and across the slices. This gives non-square pixels in the reconstructed images, but has the advantage that the IFU foreoptics will probably consist of a single spherical mirror (cf. anamorphic magnification, in which the foreoptics would include a minimum of two toroidal surfaces). The main disadvantage is that the image would be either under- or over-sampled in one dimension.

5.6. Spectrometers

The spectrometers are an Ebert-Fastie design (input and output f/10), operating over a wavelength range of $0.8\text{--}2.5\text{ }\mu\text{m}$, with a $2\text{k} \times 2\text{k}$ detector array. Two gratings provide the different spectral resolutions. In the high-resolution mode, the critically-sampled coverage in one exposure will range from $0.05\text{ to }0.2\text{ }\mu\text{m}$, depending on the central wavelength. In the low-resolution mode, either J , H , K , or $I + Z$ is covered in an exposure. The optical concept is shown in Figures 4 and 5.

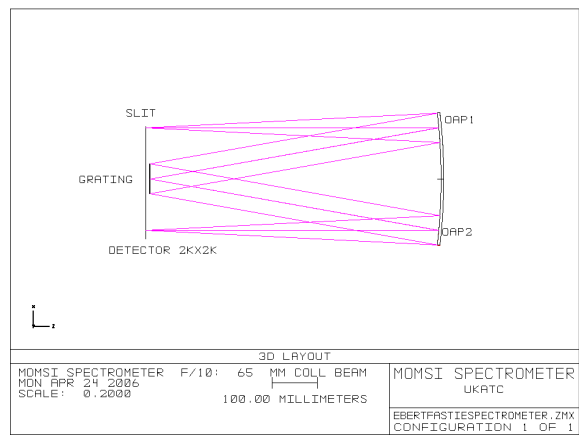


Figure 4. Ebert-Fastie spectrometer (XY-plane).

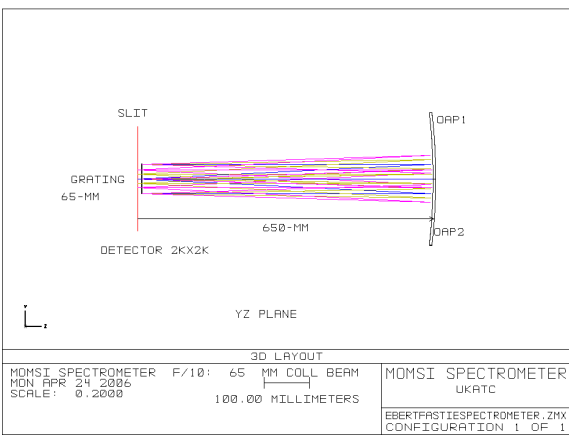


Figure 5. Ebert-Fastie spectrometer (YZ-plane).

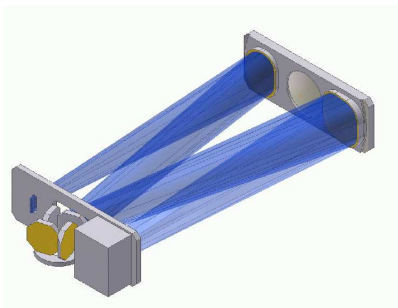


Figure 6. Mechanical design of spectrometer unit.

The mechanical concept for the spectrometer units is shown in Figure 6. Each spectrometer is 600mm long, 360mm wide and 130mm deep. The collimator and camera mirrors are identical off-axis parabolas, cut from a single substrate.

The gratings are used in first-order and are mounted on a turntable to switch between the two resolutions. The ring of 20 spectrometers is shown in Figure 7 and has an outer diameter of 1600mm.



Figure 7. Spectrometer layout.

5.7. Imagers

The imagers employ an Offner relay design (as shown in Figure 8), with a 2k×2k detector array. These will also operate over a wavelength range of 0.8-2.5 μm .

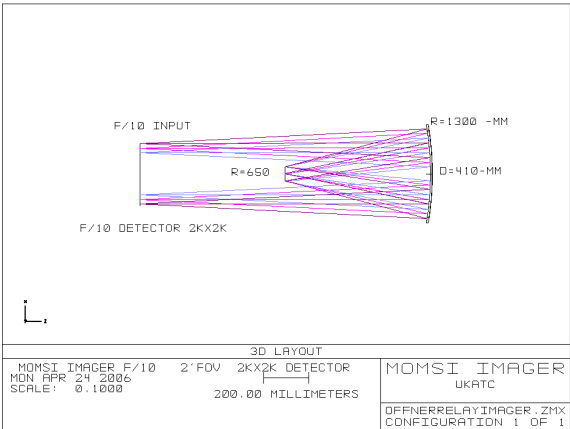


Figure 8. Offner relay imager.

6. SUMMARY

We have presented an initial design concept for a multiplexed near-IR instrument for an E-ELT, together with illustrative science cases for resolved stellar populations and galaxy evolution. The concept presented here employs pick-off arms similar to those developed for VLT-KMOS. These direct the science sub-fields to DMs for AO-correction, then onto image slicers for IFU spectroscopy, or to imaging cameras.

As with other ELT studies, the area in which the most development and effort is required is with regard to expected AO performance. As the programme for an E-ELT advances, further simulations of MOAO are required – in terms of the number of LGS/NGS required for a given AO-correction, and also in conjunction with modelling of potential science targets e.g. consideration of crowding effects in distant stellar populations. These will be incorporated into detailed point-design studies in the near future.

ACKNOWLEDGMENTS

This activity is supported by the European Community (Framework Programme 6, ELT Design Study, Contract Number 011863). We thank the staff at the Isaac Newton Group in La Palma for use of the M100 image.

REFERENCES

1. I. M. Hook, ed., *The science case for the European Extremely Large Telescope*, OPTICON, 2005.
2. E. Tolstoy in *The Scientific Requirements for Extremely Large Telescopes*, P. Whitelock, B. Leibundgut, and M. Dennefeld, eds., IAU Symposium No. 232, Cambridge University Press, 2006. astro-ph/0604065.
3. M. Steinmetz in *GAIA Spectroscopy: Science and Technology*, U. Munari, ed., p. 381, ASP Conference Series vol. 298, San Francisco, 2003.
4. R. Ibata et al. *MNRAS* **351**, p. 117, 2004.
5. A. M. N. Ferguson, M. J. Irwin, R. A. Ibata, G. F. Lewis, and N. R. Tanvir *AJ* **124**, p. 1452, 2002.
6. D. Minniti, A. A. Zijlstra, and M. V. Alonso *AJ* **117**, p. 881, 1999.
7. L. J. Smith and J. S. Gallagher *MNRAS* **326**, p. 1027, 2001.
8. G. A. Vázquez et al. *ApJ* **600**, p. 162, 2004.
9. C. J. Evans et al. *A&A* **437**, p. 467, 2005.
10. A. Kaufer, K. Venn, E. Tolstoy, C. Pinte, and R.-P. Kudritzki *AJ* **127**, p. 2723, 2004.
11. T. Repolust, J. Puls, M. M. Hanson, R.-P. Kudritzki, and M. R. Mokiem *A&A* **440**, p. 261, 2005.
12. J. S. Vink and A. de Koter *A&A* **442**, p. 587, 2005.
13. P. A. Crowther and L. J. Hadfield *A&A* **449**, p. 711, 2006.
14. J. J. Eldridge, F. Genet, F. Daigne, and R. Mochkovitch *MNRAS* **367**, p. 186, 2006.
15. Y. I. Izotov and T. X. Thuan *ApJ* **616**, p. 768, 2004.
16. M. Tecza et al. *ApJ* **605**, p. L109, 2004.
17. A. Pope et al. *MNRAS* **358**, p. 149, 2005.
18. J. Magorrian et al. *AJ* **115**, p. 2285, 1998.
19. N. Häring and H.-W. Rix *ApJ* **604**, p. L89, 2005.
20. K. Gebhardt et al. *ApJ* **543**, p. L5, 2000.
21. R. Bender et al. *ApJ* **631**, p. 280, 2005.
22. I. Trujillo, J. A. L. Aguerri, C. M. Gutiérrez, and J. Cepa *AJ* **122**, p. 38, 2001.
23. M. Giavalisco, C. C. Steidel, and F. D. Macchetto *ApJ* **470**, p. 189, 1996.
24. L. Origlia, R. M. Rich, and S. Castro *AJ* **123**, p. 1559, 2002.
25. I. Hunter et al. *A&A*, 2006. in press.
26. F. Assémat et al. *Proc. SPIE* **5237**, p. 211, 2004.
27. F. Assémat, E. Gendron, and F. Hammer *MNRAS*, 2006. in press.
28. T. J. Hawarden et al., “The provision of atmospheric dispersion correction for AO-corrected 50-m and 100-m ELTs,” (FP6 Work Package 11300: ELT-TRE-UKA-11300-00002), 2006.
29. R. M. Sharples et al. *Proc. SPIE* **5492**, p. 1179, 2004.
30. M. Wells, P. R. Hastings, and S. K. Ramsay-Howat *Proc. SPIE* **4008**, p. 1215, 2000.
31. D. Lee, C. J. Dickson, P. R. Hastings, M. Wells, and M. Leclerc *Proc. SPIE* **5494**, p. 176, 2004.